ISME

Introduced a Modified Set of Boundary Condition of Lattice Boltzmann Method Based on Bennett Extension in Presence of Buoyancy Term Considering Variable Diffusion Coefficients

M. Varmazyar[*]
Assistant Professor

M.R. Habibi[†]
Assistant Professor

A. Mohammadi[‡]
Assistant Professor

S.R. Hamzeloo[§]
Assistant Professor

Various numerical boundary condition methods have been proposed to simulate various aspects of the no-slip wall condition using the Lattice Boltzmann Method. In this paper, a new boundary condition scheme is developed to model the no-slip wall condition in the presence of the body force term near the wall which is based on the Bennett extension. The error related to the new model is smaller than those of other boundary condition methods existing in the last studies. Based on the computational results, the body forces method which representing minimum error has been illustrated. Finally, the effect of the variation of diffusion coefficients on Rayleigh-Benard convection was studied. The critical Rayleigh number, which is obtained by current method, are in good agreement with the results calculated by the linear stability theory. It has been revealed that the proposed model is capable of computing the effect of high nonlinearity in the conservative equation in the presence of variable diffusion coefficients.

Keywords: Lattice Boltzmann Method, Boundary Condition, Bennett extension, Variable Diffusion Coefficients, Rayleigh-Benard Convection

1 Introduction

Ancient models in computational fluid dynamics (CFD) are founded on the straight discretization of conservation of momentum and energy equations. These techniques have a macroscopic approach in the field of fluid dynamics simulations. On the other hand, the kinetic techniques for CFD, like the lattice Boltzmann method, take a microscopic approach and are derived from the Boltzmann equation [1-4]. One particular application of the lattice Boltzmann method is to simulate fluid under the influence of body force. Some cases of such flows are magneto-hydrodynamic fluid flow [5], buoyancy driven flow [6], multi-phase or multi-

[*] Corresponding Author, Assistant Professor, Department of Mechanical Engineering, Shahid Rajaee Teacher Training University, Shahid Shabanloo Ave, Tehran, Iran, varmazyar.mostafa@srttu.edu
[†] Assistant Professor, Energy Technological Research Division, Research Institute of Petroleum Industry (RIPI), Tehran, Iran, habibimr@ripi.ir
[‡] Assistant Professor, Department of Mechanical Engineering, Shahid Rajaee Teacher Training University, Shahid Shabanloo Ave, Tehran, Iran, amohammadi@dena.kntu.ac.ir
[§] Assistant Professor, Department of Mechanical Engineering, Shahid Rajaee Teacher Training University, Shahid Shabanloo Ave, Tehran, Iran, rehamzeloo@srttu.edu

component fluid flows [7, 8] and the flow of non-ideal gases obeying a van der Waals type of equation of state [9, 10]. Different schemes which is used to simulate the body forces are allocated into three groups. The first approach, called Scheme 1 in this study, is based on the suggestion of Luo [11] in which the effect of body forces are considered in the collision term as

$$\tilde{\mathrm{F}}_{\mathrm{i}} = -\frac{1}{c_s^2} w_i \rho \vec{c}_i . \vec{F} \tag{1}$$

Another method, referred to as Scheme 2 in the current study, is based on the work of Shan and Chen [12]. In order to account for body forces, they employed Newton's second law and modified the fluid and equilibrium velocities as follows.

$$\vec{u}(\vec{r},t) = \vec{u}'(\vec{r},t) + \tau \frac{\vec{F}(\vec{r},t)}{\rho} \tag{2}$$

$$\vec{u}^{eq}(\vec{r},t) = \vec{u}'(\vec{r},t) + \tau \frac{\vec{F}(\vec{r},t)}{\rho} \tag{3}$$

It seems to be more accurate if both the collision term and the velocity equations are modified in order to account for external forces. This idea has been employed by Guo et al. [13] and forms what is called Scheme 3 in this study. This method leads to the same conservation equations reached by macroscopic solutions. To obtain the Navier-Stokes equations, Guo et al. [13] applied the following modifications in the force and velocity equations.

$$\tilde{\mathrm{F}}_{\mathrm{i}} = \left(1 - \frac{1}{2\tau}\right) w_i \left[\frac{\vec{c}_i - \vec{u}}{c_s^2} + \frac{(\vec{c}_i . \vec{u})}{c_s^4} \vec{c}_i\right] . \vec{F} \tag{4}$$

$$\vec{u}(\vec{r},t) = \vec{u}'(\vec{r},t) + \frac{\vec{F}(\vec{r},t)}{2\rho} \tag{5}$$

$$\vec{u}(\vec{r},t) = \vec{u}'(\vec{r},t) + \frac{\vec{F}(\vec{r},t)}{2\rho} \tag{6}$$

More recently, Mohamad and Kuzmin [14] examined a good number of formulations suggested by various investigators to assess the accuracy of different schemes. They showed that the method of Guo et al. [13] is noticeably more accurate than those of others.

One of the best examples of body force is buoyancy force. To study a buoyancy-driven flow, the temperature distribution necessities to be calculated. The kinematic viscosity and the thermal diffusivity is considered changing with temperature in current study. Hazi and Markus [15] used Scheme 1 to investigate convective heat transfer to a supercritical fluid. The fluid thermal diffusivity varied with the temperature near the critical region. More recently, Varmazyar and Bazargan [16] used a Chapman-Enskog analysis and illustrated that this model can simulate the influence of nonlinearity due to the variation of thermal diffusivity in the energy equation. Recently, the effects of the body forces schemes has been investigated by Varmazayar et al. [17].The boundary conditions, as well as the body forces schemes necessity to be adjusted accordingly. The set of boundary conditions may be classified in terms of the order of magnitude of the error produced [18]. Since the accuracy of the LBM is of the second order inside the mesh points, the first order boundary conditions degrade the lattice Boltzmann method. Many efforts have been made to present higher order schemes for boundary conditions [19-23]. The bounce-back approach satisfies the mass conservation on the wall and assures the zero velocity on the boundary. However, a problem appears once the body forces are present.

They may cause a jump in the distribution function on the boundary. This has also been addressed by Li and Tafti [24] and Varmazyar et al. [17].
They showed that applying the common bounce-back boundary condition leads to an erroneous velocity jump at the wall in the presence of local forces due to liquid-vapor interactions. They developed a mass-conserving velocity-boundary condition in order to eliminate the unwanted velocity component. In current study, a new boundary condition proposed to remove the effect of the body forces near the wall which is based on the Bennett method.
To accomplish the goals mentioned above, the following steps are taken. First, the mathematical models for the fluid motion and the thermal heat transfer are presented. Then, numerical examples are applied to show the capability of the models. Next, the accuracy of the introduced boundary condition in the current study as well as various schemes used for body forces is evaluated in Poiseuille flow and Rayleigh-Benard convection case studies. Finally, the effect of variable kinematic viscosity on primary instability is investigated.

2 Governing Equations and Modeling

The LBM for an incompressible gas and corresponding thermal LBM have been described below. The variation of thermal diffusivity with temperature has been considered. Multi relaxation time scheme has been used to increase the stability and accuracy of the model.

2.1. Lattice Boltzmann Method

The lattice Boltzmann equation (LBE) is directly derived from the Boltzmann equation by discretization in both time and phase space [25]. The general form of the lattice Boltzmann equation in the i^{th} direction with body forces included is

$$f_i(\vec{r}+\vec{c}_i\ ,t+1)-f_i\ (\vec{r},t)=\Omega_i+\tilde{F}_i \tag{7}$$

where $\vec{r}$, t and $\tilde{F}_i$ are the location vector, time and body forces respectively. The term f_i is the particle distribution function traveling with velocity $\vec{c}_i$. The collision operator Ω_i represents the rate of change of f_i due to collision of particles. The particle distribution after propagation is relaxed towards the equilibrium distribution $f_i^{eq}(\vec{r},t)$. The formulation of the Bhatnagher-Gross-Krook method (BGK) [26] for collision operator has been used in this study as

$$\Omega_i=\frac{1}{\tau}(f_i\ (\vec{r},t)-f_i^{eq}(\vec{r},t)) \tag{8}$$

The relaxation parameter τ has been calculated from the kinematic viscosity υ, which is varied by temperature, according to the following equation [16].

$$\tau=3\upsilon+\frac{1}{2} \tag{9}$$

The equilibrium density $f_i^{eq}(x,t)$ is calculated as [16]

$$f_i^{eq}(\vec{r},t)=w_i\,\rho(\vec{r},t)\times(1+\frac{\vec{c}_i\,\vec{u}^{eq}}{c_s^2}+\frac{\left(\vec{c}_i\,\vec{u}^{eq}\right)^2}{2c_s^4}-\frac{\vec{u}^{eq}\,\vec{u}^{eq}}{2c_s^2}) \tag{10}$$

where c_s is the speed of sound, and w_i is the corresponding equilibrium density for $\vec{u}^{eq}=0$.
Taking the moment of the distribution function, the density and microscopic velocity may be obtained as follows [16].

$$\rho(\vec{r},t)=\sum_{\mathrm{i}}\mathrm{f}_{\mathrm{i}}\ (\vec{r},t) \tag{11}$$

$$\vec{u}'(\vec{r},t)=\frac{1}{\rho(\vec{r},t)}\sum_{\mathrm{i}}\mathrm{f}_{\mathrm{i}}\ (\vec{r},t)\vec{c}_i \tag{12}$$

The body force in the lattice Boltzmann model is calculated as below.

$$\vec{F}=\left(\rho-\rho_m\right)\vec{G} \tag{13}$$

where ρ_m and $\vec{G}$ are the average fluid density and gravity acceleration respectively. Using the Boussinesq approximation, the body force (buoyancy) term in Rayleigh-Benard convection will be

$$\vec{F}=-\rho\beta(T-T_m)\vec{G} \tag{14}$$

where T_m and β are the average fluid temperature and volumetric thermal expansion coefficients respectively.

2.2. Multi-Relaxation Time Scheme

A Multi-Relaxation Time (MRT) scheme has been applied in which the collision operator has the form of a diagonalizable matrix Ω_{ij} . The MRT collision operator interacts with equilibrium particle distribution functions as below.

$$\mathrm{f}_{\mathrm{i}}(\vec{r}+\vec{c}_i\ \ ,\mathrm{t}+1)\text{-}\mathrm{f}_{\mathrm{i}}\ (\vec{r},\mathrm{t})=-\sum_{j}\Omega_{ij}\left(\mathrm{f}_{\mathrm{j}}\ (\vec{r},\mathrm{t})\text{-}\mathrm{f}_{\mathrm{j}}^{\mathrm{eq}}\ (\vec{r},\mathrm{t})\right)+\tilde{\mathrm{F}}_{\mathrm{i}} \tag{15}$$

It has been claimed that the MRT scheme proposes a higher stability and accuracy than a single relaxation time scheme [27]. Hence, Equation (15) can be converted to the following equation.

$$\mathrm{f}_{\mathrm{i}}(\vec{r}+\vec{c}_i\ \ ,\mathrm{t}+1)\text{-}\mathrm{f}_{\mathrm{i}}\ (\vec{r},\mathrm{t})=-M^{-1}\Lambda\left(\tilde{\mathrm{f}}_{\mathrm{j}}\ (\vec{r},\mathrm{t})\text{-}\tilde{\mathrm{f}}_{\mathrm{j}}^{\mathrm{eq}}\ (\vec{r},\mathrm{t})\right)+\tilde{\mathrm{F}}_{\mathrm{i}} \tag{16}$$

where $\tilde{\mathrm{f}}_{\mathrm{j}}\ (\vec{r},\mathrm{t})$ and $\tilde{\mathrm{f}}_{\mathrm{j}}^{\mathrm{eq}}(\vec{r},\mathrm{t})$ are the vectors of the moment. The mapping between the distribution function and moment vectors can be stated by the linear transformation shown below.

$$\mathrm{f}(\vec{r},\mathrm{t})=M\ \tilde{\mathrm{f}}(\vec{r},\mathrm{t}) \tag{17}$$

The Gram-Schmidt orthogonalization procedure may be employed to calculate the transformation matrix *M*. The general form of the transformation matrix has been suggested by Ginzburg [28]. Consequently, the transformation matrix *M* for a D2Q9 type of lattice using an MRT model is expressed as below.

$$M=\begin{bmatrix}
+1 & +1 & +1 & +1 & +1 & +1 & +1 & +1 & +1\\
-4 & -1 & -1 & -1 & -1 & +2 & +2 & +2 & +2\\
+4 & -2 & -2 & -2 & -2 & +1 & +1 & +1 & +1\\
0 & +1 & 0 & -1 & 0 & +1 & -1 & -1 & +1\\
0 & -2 & 1 & +2 & 0 & +1 & -1 & -1 & +1\\
0 & 0 & +1 & 0 & -1 & +1 & +1 & -1 & -1\\
0 & 0 & -2 & 0 & +2 & +1 & +1 & -1 & -1\\
0 & +1 & -1 & +1 & -1 & 0 & 0 & 0 & 0\\
0 & 0 & 0 & 0 & 0 & +1 & -1 & +1 & -1
\end{bmatrix} \tag{18}$$

The relaxation matrix Λ used in Equation (14) is a diagonal matrix and is described as below [29].

$$\Lambda = DIAGONAL\left(0.0,\ 1.63,\ 1.14,\ \Lambda_4,\ 1.92,\ \Lambda_6,\ 1.92,\ \frac{2}{1+6\mu},\ \frac{2}{1+6\mu}\right) \tag{19}$$

where μ is the viscosity. Here, Λ_4 and Λ_6 are arbitrary values. The values of equilibrium of the moment $\tilde{f}^{eq}$ are listed below.

$$\begin{aligned}
\tilde{f}_1^{eq} &= \rho \\
\tilde{f}_2^{eq} &= -2\rho + 3\left(\vec{u}'.\vec{u}'\right) \\
\tilde{f}_3^{eq} &= \rho - 3\left(\vec{u}'.\vec{u}'\right) \\
\tilde{f}_4^{eq} &= \rho u'_x \\
\tilde{f}_5^{eq} &= -\rho u'_x \\
\tilde{f}_6^{eq} &= \rho u'_y \\
\tilde{f}_7^{eq} &= -\rho u'_y \\
\tilde{f}_8^{eq} &= \left(\rho u'_x\right)^2 - \left(\rho u'_y\right)^2 \\
\tilde{f}_9^{eq} &= \rho^2 u'_x u'_y
\end{aligned} \tag{20}$$

where u'_x and u'_y are the components of microscopic velocity.

2.3. Thermal LBM with Variable Thermal Diffusivity

To simulate the energy equation with variable thermal conductivity, the general form of the LBE has been used. To account for variations in conductivity in the heat transfer equation, the equilibrium distribution function needs to be modified as below [16].

$$g_i^{eq}(\vec{r},t) = w_i\left(T + \frac{1}{c_s^2}\rho\vec{c}_i.\vec{u} - \frac{D}{c_s^2}\vec{c}_i.\vec{\nabla}T\right) \tag{21}$$

where D is the variable part of the thermal diffusivity and T is the temperature. The relaxation time (λ) is related to the constant part of the diffusion coefficient with equation (22).

$$\lambda = \frac{1}{c_s^2}\alpha_0 + \frac{1}{2} \tag{22}$$

where α_0 is the constant part of thermal diffusivity. The Temperature is calculated by equation (23).

$$T = \sum_i g_i(\vec{r},t) \tag{23}$$

2.4. Boundary Conditions

For the Dirichlet boundary condition in thermal LBM, it is assumed that the flux is balanced in any direction ($g_i - g_i^{eq} = g_j - g_j^{eq}$). The subscript i shows the direction of particles after being reflected back to the domain. Subscript j shows the corresponding mirror direction of particles. For nodes on the wall, the balanced flux can be written as $g_i = (w_i + w_j)T_w - g_i^{eq}$ in which T_w is the wall temperature.

The introduced hydrodynamic boundary condition in this study is based on the Bennett extension. The moment-based model of Bennett [30] is a generalization of the method of Noble et al. [22] which formulates the boundary conditions in terms of the moments of the distribution functions, rather than on the distribution functions directly. In the moment-based approach, the nine independent moments can be defined as below.

$$m = \left(\Pi_0, \Pi_X, \Pi_Y, \Pi_{XX}, \Pi_{YY}, \Pi_{XY}, \Pi_{XYY}, \Pi_{XXY}, \Pi_{XXYY}\right) \tag{24}$$

where m may be expressed in the computational scale as $m = M' \times \mathrm{f}$ and M' is a transform matrix defined as follows.

$$M' = \begin{pmatrix} 1 & 1 & 1 & 1 & 1 & 1 & 1 & 1 & 1 \\ 0 & 1 & 0 & -1 & 0 & 1 & -1 & -1 & 1 \\ 0 & 0 & 1 & 0 & -1 & 1 & 1 & -1 & -1 \\ 0 & 1 & 0 & 1 & 0 & 1 & 1 & 1 & 1 \\ 0 & 0 & 1 & 0 & 1 & 1 & 1 & 1 & 1 \\ 0 & 0 & 0 & 0 & 0 & 1 & -1 & 1 & -1 \\ 0 & 0 & 0 & 0 & 0 & 1 & -1 & -1 & 1 \\ 0 & 0 & 0 & 0 & 0 & 1 & 1 & -1 & -1 \\ 0 & 0 & 0 & 0 & 0 & 1 & 1 & 1 & 1 \end{pmatrix} \tag{25}$$

By this approach, the boundary condition method can be categorized. In the current study, a new boundary condition based on Allen and Reis approach [31] are proposed by using the moment-based model of Bennett method. In this scheme, it is assumed that the solid boundaries are impermeable, rigid and stationary, and subjected to the no–slip condition. For calculating the three unknowns in each horizontal wall in terms of the moment constraints and the known distributions, it is required to consider three equations. The unknown values of f_2, f_5, and f_6 pointing outwards with respect to the southern wall are to be calculated by using the after streaming values of f_0, f_1, f_3, f_4, f_7, f_8.

In order to implement the conservative momentum equations in computational domain, it is required to take the hydrodynamic moments. It consists of two components of momentum (Π_X, Π_Y) and the remaining independent component of the momentum flux (Π_{XXY}).

In current boundary condition scheme, to simulate the zero velocity on the wall, a bounce-back type of boundary condition on the non-equilibrium part of the distribution function is implemented. Figure (1) is presented to explain the boundary condition used in the current study. The south wall is coinciding with the x-axis and is shown by the dotted line in Figure (1). Accordingly, the equations are set as below to obtain the unknown variables in the current scheme.

$$\Pi_X = 0 \qquad \Pi_Y = -F_y / 2 \qquad \Pi_{XXY} = -F_y / 2 \tag{26}$$

By considering the southern boundary and using the above system of equations, we can calculate the unknown distribution function at the south wall. Finally, the equations above are employed to determine f2, f5, and f6 as follows.

$$\mathrm{f}_2 = \mathrm{f}_4 - 2\rho u_y / 3 \tag{27}$$

$$f_5 = f_7 + (f_1 - f_3)/2 + F_y/4$$
$$f_6 = f_8 - (f_1 - f_3)/2 + F_y/4$$

3 Results and Discussion

To illustrate the capabilities of the present model, two examples are numerically simulated. At first case, the three schemes of body forces are applied in a Poiseuille flow with modified boundary condition which have been studied and the errors of all results are compared. In the next case, a Rayleigh-Benard convection problem is simulated. Stability analysis in various conditions as well as the accuracy of solution in each simulation are investigated. In this case study, thermal diffusivity is considered varied with temperature.

3.1. Poiseuille Flow Case Study

One of the best case studies could be selected for the assessment of the present model was a Poiseuille flow driven, due to its known analytical solution. From the Navier-Stokes equations for incompressible Poiseuille flow, the velocity profile could be extracted as follows.

$$u_y = u_0\left(1-\left(\frac{2y}{Ly}\right)^2\right) \tag{28}$$

where in $u_0 = F_d Ly^2/(4\rho\upsilon)$, F_d is the driving force and Ly is the channel width. The effect of channel width on error variations is studied. Various grid resolutions from Ly=8 to Ly=64 have been tried. The constant Reynolds number $Re=u_0Ly/\upsilon$ has been considered. The product u_0Ly remained constant because the kinematic viscosity depends only on τ. The no-slip boundary condition on the top and bottom boundaries is used. Also periodic boundary condition along flow direction is assigned to inlet and outlet boundaries. The error function is defined as Equation (29).

$$err = \sqrt{\sum_i (UN_i - UE_i)^2 / N_n} \tag{29}$$

Where N_n is the number of points, UE_i and UN_i are correspond to the analytical and numerical normalized velocity for the ith node, respectively. The velocity is normalized with the velocity in the canter of channel. Figure (2) shows that the numerical error decreases by increasing the channel width. However, the values of resulted error of the present model are approximately same as the results obtained in [17] and too smaller in comparison with the errors obtained by Chen et al [18].

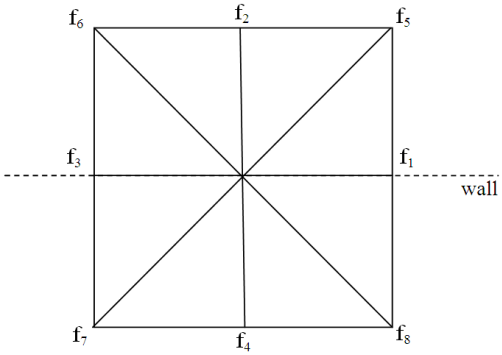

Figure 1 Distribution function for D2Q9 configuration on the upper wall

3.2. Rayleigh-Benard Convection Case Study

A two-dimensional simulation of steady Rayleigh-Benard natural convection has been considered to assess the present models. The diagram of the flow between two parallel plates and the macroscopic boundary conditions are illustrated as a schematic in Figure (3). The walls at $y = 0$ and $y = Ly$ are heated and cooled respectively. Other walls are in periodic conditions. The fluid is initially at rest. Thermodynamic equilibrium at constant temperature T_0 is maintained. T_0 is the average of the heated and cooled wall temperatures. The variation of the thermal diffusivity has been estimated by a linear equation as stated below.

$$\alpha_0 + D(T) = \frac{k_0 + k(T)}{\rho c_p} = \alpha_0 \left[1 + \gamma \left(T - T_{bottom}\right)\right] \tag{30}$$

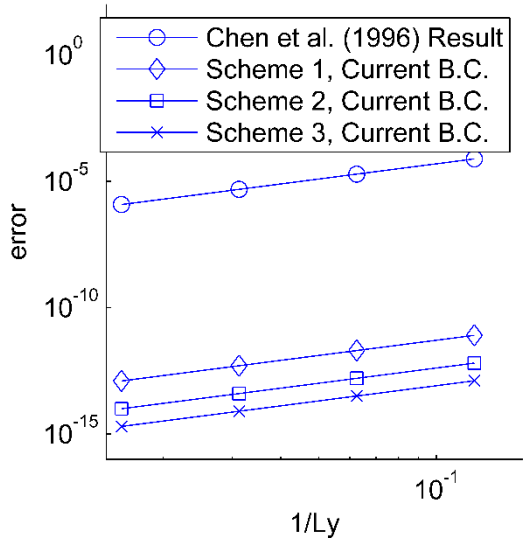

Figure 2 Error respected to channel width for Poiseuille flow

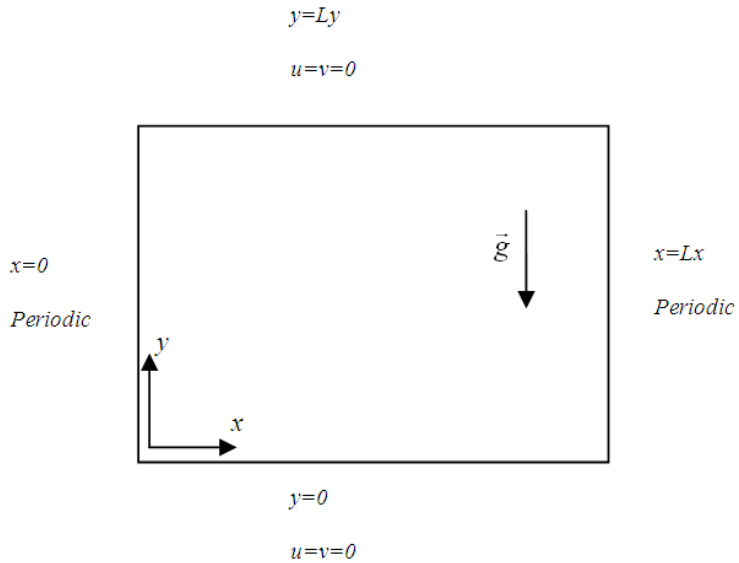

Figure 3 Distribution function for D2Q9 configuration on the upper wall

In the Equation (30), $k(T)$, ρ and c_p are the thermal conductivity, the density and the specific heat capacity respectively. To calculate the temperature distribution and velocity profiles, the D2Q9 is used. To investigate the independency of the numerical solution from the number of grids, different lattice sizes from 31×61 to 151×301 are examined. It was observed that there is no significant difference in the results with the number of grids larger than 111×221. Calculations at different Rayleigh numbers are accomplished on a 111×221 lattice with a Prandtl number of 0.71.

The simulation is taking place from the static conductive state, starting with Ra=2,000. The Nusselt numbers simulated under the steady-state situations and constant diffusion coefficient are illustrated in Table (1). Two flows with different Rayleigh numbers are studied. The results of different schemes for modeling body forces as well as the various models for boundary condition including the one proposed in this study are presented in This Table. The results of a semi-empirical correlation, $Nu=1.56\times(Ra/Rac)^{0.296}$ with critical Rayleigh number (Rac) equal to 1707, are also showed for the sake of comparison. Comparison of the calculated results with the semi-empirical correlation show that applying scheme 3 for the current boundary condition yields the least amount of error.

For a wide range of Rayleigh numbers, the steady-state streamlines and isotherms are shown in Figure (4). As it is observable, increasing the Rayleigh number leads to the smaller thickness of thermal boundary layer. Also, the rising and falling fluid layers become narrower. The Rayleigh number is increased to magnitudes as high as 1,000,000. Unlike the thermal LBE model [32], the present model remains numerically stable.

In the next assessment, the variation of thermal diffusivity has been taken into account. The calculations have been carried out by considering various values of the thermal diffusivity coefficient, $\gamma = 0.2$, 0.4 and 0.6. The Ra and Pr numbers are assumed to be 1,000,000 and 0.71 respectively. The isotherms for various values of γ are illustrated in Figure (5). The calculated corresponding Nusselt Numbers for Ra=500,000 and Ra=1,000,000 are presented in Table (2) with $\gamma = 0.0$, 0.1, 0.3, 0.5 and 0.7. As illustrated in the Figure (5), an increment in the thermal diffusivity coefficient leads to the narrower thermal boundary layer. The high nonlinearity in the heat transfer equation causes to the high-temperature region near the cold wall becoming larger. Results show that the present thermal LBM can simulate highly nonlinear energy equations acceptably.

3.3 Primary Instability of Rayleigh Benard Convection

At first, the presented lattice Boltzmann method was validated by considering the case of the primary instability of Rayleigh-Benard convection with constant properties. Using the linear stability theory, the exact values of critical wave number and critical Rayleigh number, for constant property Rayleigh–Benard convection with rigid bodies are obtained to be 3.117 and 1707.8 respectively [33].

Table 1 Nusselt number calculated by numerical schemes and semi empirical correlation for a Rayleigh-Benard convection problem

Scheme used to model body force	Boundary condition modeling	Nusselt Number	
		Ra=20,000	Ra=30,000
Scheme 3	First Order Bounce-Back	3.247	3.564
Scheme 3	Second Order Bounce-Back	3.210	3.565
Scheme 1	Current model	3.228	3.607
Scheme 2	Current model	3.791	4.219
Scheme 3	Current model	3.236	3.639
Semi empirical correlation: $1.56\times(Ra/Rac)^{0.296}$		3.232	3.644

According to this critical wave number, the aspect ratio AR = Lx/Ly is considered $2\pi/3.117 \cong 2$. To investigate the grid independency, several different grid sizes, 81x41, 161x81, 321x161 and 641x321 have been examined. The estimated critical Rayleigh numbers at different grid sizes are calculated. It can be deduced that the increase of the grid size beyond 81x41 does not have a significance effect on the accuracy of the results and the critical Rayleigh number is obtained 1707. The critical Rayleigh number is calculated by the interpolation between the growth rate and the decay rate of maximum vertical velocity in various Rayleigh numbers. The same grid size has been employed in previous studies [34-36] for 2D channel flow discretized by the square lattice using D2Q9 model. From the results calculated, it also can be seen that the value of critical Rayleigh number is independent of the Prandtl number.
Richardson and Straughan [37] employ a nonlinear energy stability theory for the onset of convection for a fluid with kinematic viscosity depending linearly on temperature. They prove that the eigenvalue models which is obtained from the nonlinear theory is exactly the same as the one of linear instability theory arising from the conservation equations and thus the critical Rayleigh numbers that are resulted from the linear instability and the nonlinear energy stability are the same. They solved numerically the eigenvalue problem with the compound matrix method for free surface boundary condition and state that their results have good agreement with the previous experimental data such as Richter et al. [38]. Capone and Gentile [39] repeated Richardson and Straughan study for fluids with viscosity depending exponentially on temperature. They also consider the free surface boundary condition same as Richardson and Straughan study. At first, the rigid body boundary condition has been chosen by Rajagopal et al. [40]. They employ the Galerkin method, which is utilized by Chandrasekhar [41], to study the thermal-convection instability for the fluid with a viscosity that depends exponentially on the temperature and pressure. By neglecting the pressure effect, the viscosity is assumed has an analytic function of the temperature as below:

$$\upsilon = \upsilon_0 \exp\left[\gamma'\left(T - T_{cold}\right)\right] \tag{31}$$

By considering the $Ra<Ra_c$, above equation will convert to the following equation

$$\upsilon = \upsilon_0 \exp\left[\Gamma\left(\frac{y}{Ly} - 1\right)\right] \tag{32}$$

Where Γ is equal to the $\gamma'(T_{hot} - T_{cold})$. They obtained that the critical wave number is about 3.117 to 3.072 for $|\Gamma|$ which is equal from 0 to 2.

Table 2 Nusselt number values calculated by numerical scheme with variation of thermal diffusivity

	Nusselt Number	
	Ra=500,000	Ra=1,000,000
$\gamma = 0.0$	7.641	8.719
$\gamma = 0.1$	7.726	9.139
$\gamma = 0.3$	8.168	9.694
$\gamma = 0.5$	8.614	10.173
$\gamma = 0.7$	9.103	10.787

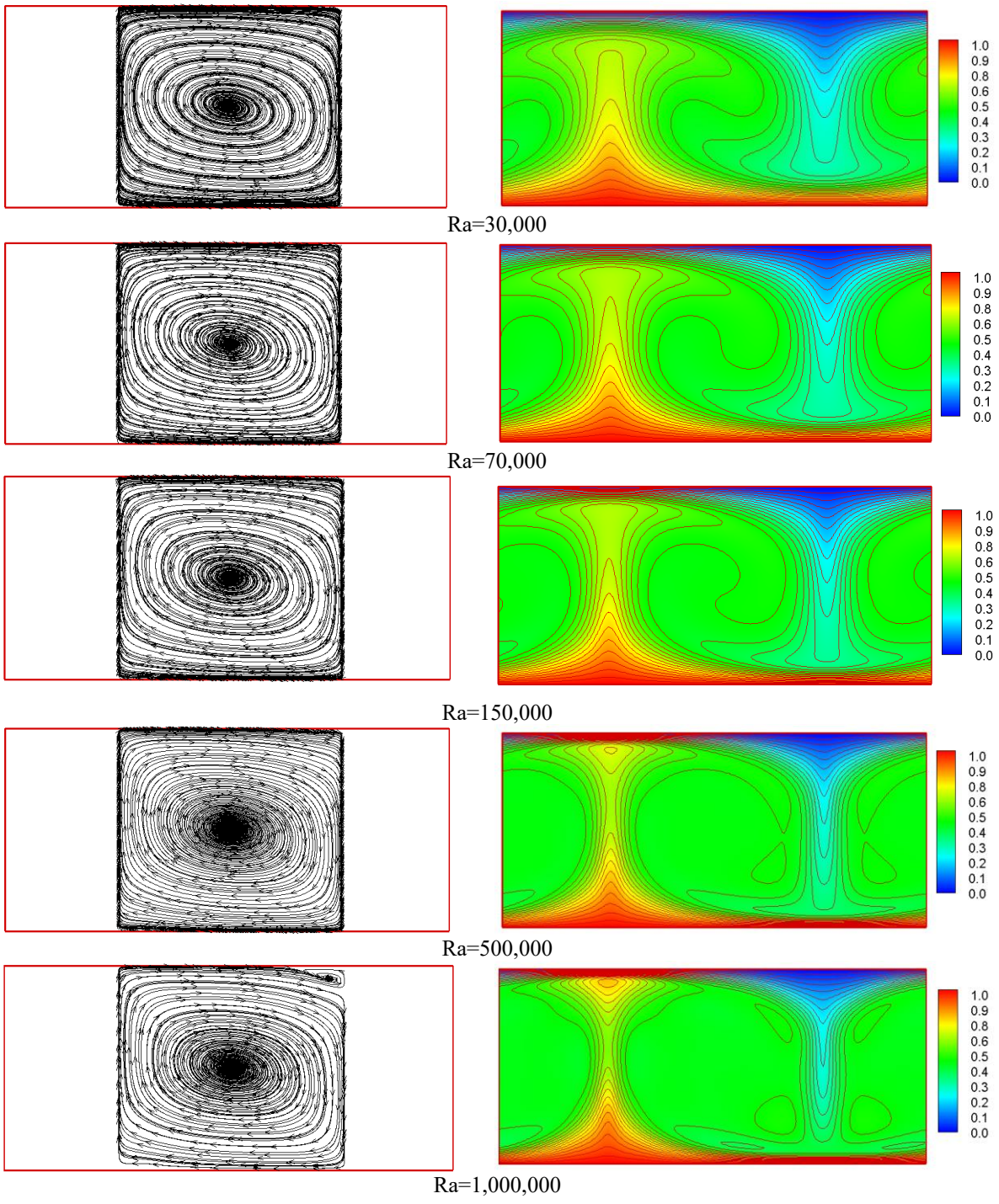

Figure 4 Two-dimensional simulation streamlines and isotherms at steady states for wide range of Rayleigh numbers

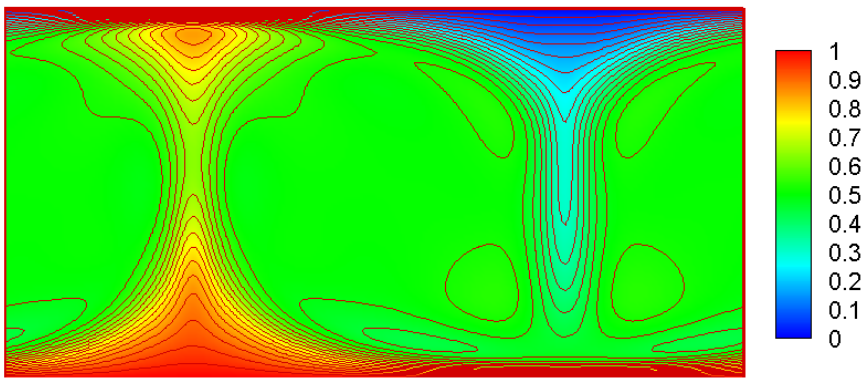

$\gamma = 0.2$

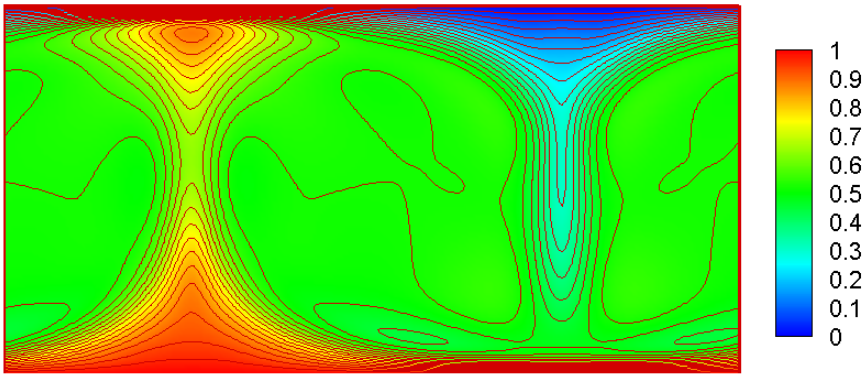

$\gamma = 0.4$

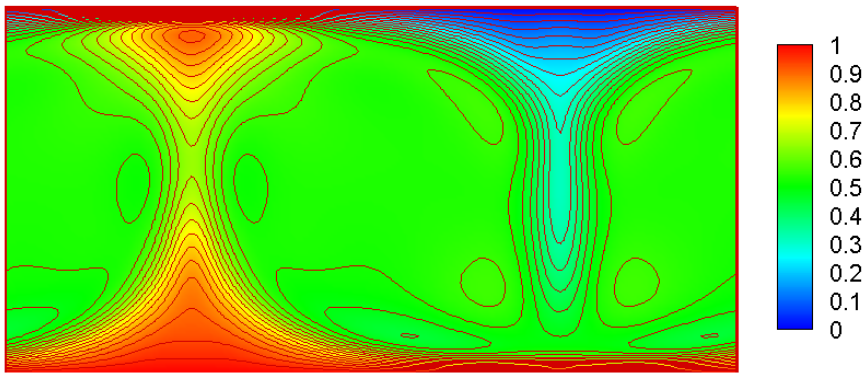

$\gamma = 0.6$

Figure 5 Two-dimensional simulation Isotherms at steady states for Ra=1,000,000 with variation of thermal diffusivity

Table 3 Critical Rayleigh number versus different Γ reported by Rajagopal et al. [40] compared with current calculated results

	critical Rayleigh number	
	Rajagopal et al. [40]	current results (Pr=0.7)
$\Gamma = -2.0$	5026.42	5015±1
$\Gamma = -1.5$	3790.86	3781±1
$\Gamma = -1.0$	2885.93	2877±1
$\Gamma = -0.5$	2217.33	2213±1
$\Gamma = +0.5$	1344.88	1349±1
$\Gamma = +1.0$	1061.67	1069±1
$\Gamma = +1.5$	845.855	854±1
$\Gamma = +2.0$	680.252	696±1

Therefore, the aspect ratio about 2.0 is until true. They used the linear as well as the non-linear stability theorem to obtain the approximations to the critical Rayleigh number for different values of the dimensionless parameter Γ. By considering the aspect ratio equal to 2, the calculated results of the lattice Boltzmann method can be comparable with the Rajagopal et al. [40] results. The critical number which is obtained from lattice Boltzmann method is divided by the Rajagopal et al. [40] results and is shown in Table (3). In Rajagopal et al. study, the fluid diffusion properties in Rayleigh number are calculated at the $\Gamma = 0$.

4 Conclusions

In this paper, a modified no-slip wall condition model has been proposed to reduce the error initiated by applying regular boundary condition method. For this purpose, a body force term near the wall has been taken into account. As demonstrated in results, the presented boundary condition method, same as the model is suggested in [17], is more accurate than previous methods in the literature.
A wide range of Rayleigh numbers has been examined in the simulation of steady-state Rayleigh-Benard convection problem by the current method. Furthermore, the effect of high nonlinearity is considered in the conservative equation by simulations applying the proposed model. To assess the current schemes, the Rayleigh-Benard convection problem simulated by considering the variable thermal diffusivity. The stability conditions obtained for flows with a large variation of thermal conductivity ($\gamma = 0.7$) and Rayleigh numbers up to 1,000,000. At the last assessment, the variable kinematic viscosity has been applied to investigate the primary instability of Rayleigh-Benard convection. The calculated results demonstrated that the current method is capable to estimate the critical Rayleigh number with high accuracy within the variation of the diffusion coefficient.

References

[1] Qian, Y., d'Humières, D., and Lallemand, P., "Lattice BGK Models for Navier-stokes Equation", EPL (Europhysics Letters), Vol. 17, No. 6, pp. 479-484, (1992).

[2] Abe, T., "Derivation of the Lattice Boltzmann Method by Means of the Discrete Ordinate Method for the Boltzmann Equation", Journal of Computational Physics, Vol. 131, No. 1, pp. 241-246, (1997).

[3] Lallemand, P., and Luo, L. S., "Theory of the Lattice Boltzmann Method: Dispersion, Dissipation, Isotropy, Galilean Invariance, and Stability", Physical Review E, Vol. 61, No. 6, pp. 6546-6562, (2000).

[4] Succi, S., "*The Lattice Boltzmann Equation: for Fluid Dynamics and Beyond*", Oxford University Press, London, United Kingdom, (2001).

[5] Aghaei, A. R., Sheikhzadeh, G. A., Khorasanizadeh, H., and Ehteram, H. R., "Effect of Magnetic Field on Heat Transfer of Nanofluid with Variable Properties on the Inclined Enclosure", Iranian Journal of Mechanical Engineering Transactions of the ISME, Vol. 15, No. 1, pp. 28-38, (2014).

[6] Varmazyar, M., Bazargan, M., Moahmmadi, A., and Rahbari, A., "Error Analysis of Thermal Lattice Boltzmann Method in Natural Convection Problems with Varying Fluid Thermal Diffusion Coefficient", Modares Mechanical Engineering, Vol. 16, No. 12, pp. 335-344, (2016).

[7] Aminfar, H., and Haghgoo, M. R., "Modeling of Upward Subcooled Flow Boiling of Refrigerant-113 in a Vertical Annulus", Iranian Journal of Mechanical Engineering Transactions of the ISME, Vol. 12, No. 1, pp. 19-40, (2011).

[8] Huang, H., Thorne Jr, D. T., Schaap, M. G., and Sukop, M. C., "Proposed Approximation for Contact Angles in Shan-And-Chen-Type Multicomponent Multiphase Lattice Boltzmann Models", Physical Review E, Vol. 76, No. 6, pp. 066701:1-6, (2007).

[9] Varmazyar, M., and Bazargan, M., "Numerical Investigation of the Piston Effect of Supercritical Fluid under Microgravity Conditions using Lattice Boltzmann Method", Modares Mechanical Engineering, Vol. 17, No. 5, pp. 138-146, (2017).

[10] Varmazyar, M., and Bazargan, M., "Modeling of Free Convection Heat Transfer to a Supercritical Fluid in a Square Enclosure by the Lattice Boltzmann Method", Journal of Heat Transfer, Vol. 133, No. 2, pp. 022501:1-5, (2011).

[11] Luo, L. S., "Lattice-gas Automata and Lattice Boltzmann Equations for Two-dimensional Hydrodynamics", Ph.D. Thesis, Georgia Institute of Technology, Atlanta, USA, (1993).

[12] Shan, X., and Chen, H., "Simulation of Nonideal Gases and Liquid-gas Phase Transitions by the Lattice Boltzmann Equation", Physical Review E, Vol. 49, No. 4, pp. 2941-2948, (1994).

[13] Guo, Z., Zheng, C., and Shi, B., "Discrete Lattice Effects on the Forcing Term in the Lattice Boltzmann Method", Physical Review E, Vol. 65, No. 4, pp. 046308:1-6, (2002).

[14] Mohamad, A., and Kuzmin, A., "A Critical Evaluation of Force Term in Lattice Boltzmann Method, Natural Convection Problem", International Journal of Heat and Mass Transfer, Vol. 53, No. 5, pp. 990-996, (2010).

[15] Házi, G., and Márkus, A., "Modeling Heat Transfer in Supercritical Fluid using the Lattice Boltzmann Method", Physical Review E, Vol. 77, No. 2, pp. 026305:1-10, (2008).

[16] Varmazyar, M., and Bazargan, M., "Development of a Thermal Lattice Boltzmann Method to Simulate Heat Transfer Problems with Variable Thermal Conductivity", International Journal of Heat and Mass Transfer, Vol. 59, pp. 363-371, (2013).

[17] Varmazyar, M., Mohammadi, A., and Bazargan, B., "Buoyancy Term Evolution in the Multi Relaxation Time Model of Lattice Boltzmann Method with Variable Thermal Conductivity using a Modified Set of Boundary Conditions", International Journal of Engineering, Vol. 30, No. 9, pp. 1408-1416, (2017).

[18] Chen, S., Martinez, D., and Mei, R., "On Boundary Conditions in Lattice Boltzmann Methods", Physics of Fluids (1994-present), Vol. 8, No. 9, pp. 2527-2536, (1996).

[19] Latt, J., "Hydrodynamic Limit of Lattice Boltzmann Equations", Thesis, Faculty of Science, University of Geneva, Switzerland, (2007).

[20] Latt, J., Chopard, B., Malaspinas, O., Deville, M., and Michler, A., "Straight Velocity Boundaries in the Lattice Boltzmann Method", Physical Review E, Vol. 77, No. 5, pp. 056703:1-16, (2008).

[21] Martys, N. S., and Chen, H., "Simulation of Multicomponent Fluids in Complex Three-dimensional Geometries by the Lattice Boltzmann Method", Physical Review E, Vol. 53, No. 1, pp. 743-751, (1996).

[22] Noble, D. R., Chen, S., Georgiadis, J. G., and Buckius, R. O., "A Consistent Hydrodynamic Boundary Condition for the Lattice Boltzmann Method", Physics of Fluids (1994-present), Vol. 7, No. 1, pp. 203-209, (1995).

[23] Skordos, P., "Initial and Boundary Conditions for the Lattice Boltzmann Method", Physical Review E, Vol. 48, No. 6, pp. 4823-4842, (1993).

[24] Li, S. M., and Tafti, D. K., "Near-critical CO2 Liquid–vapor Flow in a Sub-microchannel. Part I: Mean-field Free-energy D2Q9 Lattice Boltzmann Method", International Journal of Multiphase Flow, Vol. 35, No. 8, pp. 725-737, (2009).

[25] He, X., and Luo, L. S., "A Priori Derivation of the Lattice Boltzmann Equation", Physical Review E, Vol. 55, No. 6, pp. R6333-6336, (1997).

[26] Bhatnagar, P. L., Gross, E. P., and Krook, M., "A Model for Collision Processes in Gases. I. Small Amplitude Processes in Charged and Neutral One-component Systems", Physical Review, Vol. 94, No. 3, pp. 511-525, (1954).

[27] Mohamad, A. A., "*Lattice Boltzmann Method: Fundamentals and Engineering Applications with Computer Codes*", Springer Science & Business Media, Berlin, Germany, (2011).

[28] Ginzburg, I., "Equilibrium-type and Link-type Lattice Boltzmann Models for Generic Advection and Anisotropic-dispersion Equation", Advances in Water Resources, Vol. 28, No. 11, pp. 1171-1195, (2005).

[29] Xu, Y., Liu, Y., Xia, Y., and Wu, F., "Lattice-boltzmann Simulation of Two-dimensional Flow Over Two Vibrating Side-by-side Circular Cylinders", Physical Review E, Vol. 78, No. 4, pp. 046314:1-12, (2008).

[30] Bennett, S., "A Lattice Boltzmann Model for Diffusion of Binary Gas Mixtures", Thesis, Department of Engineering, University of Cambridge, Cambridge, England, (2010).

[31] Allen, R., and Reis, T., "A Lattice Boltzmann Model for Natural Convection in Cavities", International Journal of Heat and Fluid Flow, Vol. 76, No. 5, pp. 1-12, (2013).

[32] McNamara, G. R., and Zanetti, G., "Use of The Boltzmann Equation to Simulate Lattice-gas Automata", Physical Review Letters, Vol. 61, No. 20, pp. 2332-2335, (1988).

[33] Reid, W., and Harris, D., "Some Further Results on the Bénard Problem", Physics of Fluids (1958-1988), Vol. 1, No. 2, pp. 102-110, (1958).

[34] He, X., Chen, S., and Doolen, G. D., "A Novel Thermal Model for the Lattice Boltzmann Method in Incompressible Limit", Journal of Computational Physics, Vol. 146, No. 1, pp. 282-300, (1998).

[35] Kao, P. H., and Yang, R. J., "Simulating Oscillatory Flows in Rayleigh–benard Convection using the Lattice Boltzmann Method", International Journal of Heat and Mass Transfer, Vol. 50, No. 17, pp. 3315-3328, (2007).

[36] Xu, K., and Lui, S. H., "Rayleigh-Bénard Simulation using the Gas-kinetic Bhatnagar-Gross-Krook Scheme in the Incompressible Limit", Physical Review E, Vol. 60, No. 1, pp. 464-470, (1999).

[37] Richardson, L., and Straughan, B., "A Nonlinear Energy Stability Analysis of Convection with Temperature Dependent Viscosity", Acta mechanica, Vol. 97, No. 1-2, pp. 41-49, (1993).

[38] Richter, F. M., Nataf, H. C., and Daly, S. F., "Heat Transfer and Horizontally Averaged Temperature of Convection with Large Viscosity Variations", Journal of Fluid Mechanics, Vol. 129, pp. 173-192, (1983).

[39] Capone, F., and Gentile, M., "Nonlinear Stability Analysis of Convection for Fluids with Exponentially Temperature-dependent Viscosity", Acta Mechanica, Vol. 107, No. 1-4, pp. 53-64, (1994).

[40] Rajagopal, K., Saccomandi G., and Vergori, L., "Stability Analysis of the Rayleigh–Bénard Convection for A Fluid with Temperature and Pressure Dependent Viscosity", Zeitschrift für Angewandte Mathematik und Physik (ZAMP), Vol. 60, No. 4, pp. 739-755, (2009).

[41] Chandrasekhar, S., "*Hydrodynamic and Hydromagnetic Stability*", Courier Corporation, North Chelmsford, Massachusetts, United States, (2013).

Nomenclature

$\vec{c}_i$	lattice velocity vector in the direction *i*, m/s
c_p	specific heat capacity, kJ/kg.K
c_s	the speed of sound, m/s
D	the variable part of the thermal diffusivity, m^2/s
err	numerical error
$\mathrm{f}_i(\vec{r},t)$	particle distribution function traveling with velocity $\vec{c}_i$, kg
$\mathrm{f}_i^{eq}(\vec{r},t)$	equilibrium distribution function traveling with velocity $\vec{c}_i$, kg
$\tilde{\mathrm{f}}(\vec{r},t)$, $\tilde{\mathrm{f}}^{eq}(\vec{r},t)$	vectors of moment corresponding to $\mathrm{f}_i(\vec{r},t)$ and $\mathrm{f}_i^{eq}(\vec{r},t)$ respectively
F_d	driving force, $kg/m.s^2$

$\tilde{F}_i$	effect of the body force ($\vec{F}$) in the collision term, kg/s
$g_i(\vec{r},t)$	particle distribution function in the i^{th} direction, K
$g_i^{eq}(\vec{r},t)$	equilibrium distribution function in the i^{th} direction, K
$\vec{G}$	gravity acceleration, m/s^2
$k(T)$	the variable part of thermal conductivity,W/m.K
k_0	the constant part of thermal conductivity, W/m.K
Lx, Ly	rectangular geometry dimensions, m
m	hydrodynamic moments
M , M'	transformation matrix
N_n	number of nodes
Pr	Prandtl number ($= \upsilon / \alpha_0$)
$\vec{r}$	location vector (*x*,*y*), m
Ra	Rayleigh number
Re	Reynolds number
t	time, s
T	temperature, K
T_0	an average of the heated and cooled wall temperature, K
T_m	average fluid temperature, K
T_w	wall temperature, K
$\vec{u}$	fluid velocity vector with u_x and u_y components, m/s
$\vec{u}'$	microscopic velocity, m/s
$\vec{u}^{eq}$	equilibrium velocity, m/s
UE_i	analytical normalized velocity for ith direction node
UN_i	numerical normalized velocity for ith direction node
w_i	lattice constant in the direction *i*
x, y	coordinate axis directions

Greek symbols

α_0	the constant part of the thermal diffusivity, m^2/s
β	Volumetric thermal expansion coefficient, 1/K
γ	variable thermal conductivity parameter, 1/K
λ	relaxation time in the energy equation, s
μ	dynamic viscosity, m^2/s
ρ	density, kg/m^3
ρ_m	average fluid density, kg/m^3
τ	relaxation time in the momentum equation, s
υ	kinematic viscosity, m^2/s
Λ	relaxation matrix
Π	components of hydrodynamic moments
Ω	collision operator

چکیده

تاکنون اسکیم های متعددی در روش شبکه بولتزمن برای مدل سازی شرط عدم لغزش بر روی دیواره معرفی شده است. مطالعه حاضر به معرفی یک مدل جدید جهت اعمال شرط عدم لغزش بر روی دیواره بر اساس روش بنت درحضور نیروی حجمی می پردازد. نشان داده شد که خطای شرط معرفی شده کمتر از خطای شروط مرزی معرفی شده در مطالعات گذشته می باشد.

تاثیر اسکیم های اعمال نیروی حجمی نیز در روش شبکه بولتزمن با لحاظ شرط مرزی مذکور مورد بررسی قرار گرفت و اسکیم دارای کمترین خطا معرفی گردید. نهایتا به بررسی اثر ضریب پخش متغیر بر روی جریان رایلی بنارد با استفاده از اسکیم های مذکور پرداخته شد. عدد رایلی بحرانی محاسبه شده در توافق خوبی با نتایج محاسبه شده به کمک تیوری پایداری خطی است. لذا می توان گفت این اسکیم قابلیت مدلسازی اثرات غیرخطی از جمله تغییرات شدید ضریب پخش را دارا می باشد.